16th European Signal Processing Conference (EUSIPCO 2008), Lausanne, Switzerland, August 25-29, 2008, copyright by EURASIP

A NOVEL TECHNIQUE FOR SPIKE DETECTION IN EXTRACELLULAR NEUROPHYSIOLOGICAL RECORDINGS USING CEPSTRUM OF BISPECTRUM

Shahjahan Shahid and Leslie S. Smith

Department of Computing Science and Mathematics
University of Stirling, Stirling, FK9 4LA, Scotland, UK
phone: + 44 1786 467422, fax: + 44 1786 464551, email: ssh@cs.stir.ac.uk
web: http://www.cs.stir.ac.uk

ABSTRACT

Signals from extracellular electrodes in neural systems record voltages resulting from activity in many neurons. Detecting action potentials (spikes) in a small number of specific (target) neurons is difficult because of poor SNR due to noise generated by the firing of neighbouring neurons. A new algorithm for spike detection has been developed: it applies a Cepstrum of Bispectrum (CoB) estimated inverse filter to provide blind equalization. This CoB based technique can detect 99% of spike events with less than 1% false positives (insertions) from the extracellular signal at up to -10dB SNR. We compare performance with four established techniques and report that the CoB based algorithm performs best.

1. INTRODUCTION

The tip of an extracellular micro-electrode is generally surrounded by many neurons and so detects the sum of many neurons' electrical activities. Often it is the timing of spikes (action potentials) in different nearby neurons which is of interest. In some experiments, it may be possible to place extracellular electrodes so as to isolate a single neuron's activity, but this is not generally the case. The closest neurons result in the highest electrical activity at the tip, but surrounding neurons superimpose activity changes on the amplitude and shape of the signal of interest. Signal transfer from neuron to electrode may be resistive and/or capacitative, resulting in spikes appearing as weak signals whose shape and amplitude may differ from intracellular spike shapes because of the transfer path characteristics [15] resulting from the cell geometry, the distribution and density of ion channels and the position of the recording electrode with respect to electrically active membranes [10]. Further, the activity of distant neurons may appear as noise which is highly correlated with the target signal [4]. Finding spike trains from multiple neurons ("spike sorting") is generally a two stage task [13]: spikes are first detected, and then ascribed to a particular neuron, depending on their shape and size. This paper deals purely with signal processing for spike detection. Extracellular neural recordings are inevitably corrupted by noise from varied sources: the recording hardware, the ambient recording environment and the spatially averaged activity of distant cells [2]. All these issues make the problem of spike detection challenging.

The simplest and most widely used technique for spike detection is amplitude thresholding. This detects events when the signal crosses a user-specified single [1] (or pair of [3]) amplitude thresholds which can be set manually by visual inspection or automatically, (e.g, as some multiple of the estimated standard deviation of the signal [4]). The performance of this technique deteriorates rapidly at low SNR [16] since it does not employ any preprocessing [13]. Another drawback is that overlapping neural signals may be considered as a single neural spike or alternatively missed due to the low amplitude of the sum. This reduces the efficacy of simple threshold detection [11].

Spike detection based on a nonlinear energy operator (NEO) computes the product of the instantaneous amplitude and frequency of the extracellular signal. This enhances the spike events in the signal [8]. Since the energy computation uses signal amplitude without compensating for noise, it does not perform well on noisy signals.

Defining templates, and matching the signal with the template provides another class of technique for spike detection [5]. Automatic template selection requires amplitude or duration bootstrapping to generate approximations of actual spikes [6]. There are many available methods for determining similarity of sections of a signal, such as sum-of-squared differences [12], convolution [9], cross-correlation [7], and maximum likelihood [12]. The performance of this technique again decreases in low SNR since the automatic selection of a template in a noisy signal is very difficult. In addition, overlapping spikes may produce a novel spike shape which can worsen performance.

Recent publications using coefficients of the wavelet transform [10] have shown good performance in spike detection from neural data. The coefficients are found by carrying out a correlation function with a mother wavelet and, given a good choice of mother wavelet, the spike properties are enhanced in the coefficients produced. This transform is able to separate signals from noise so that this technique shows good performance in low SNR [16]. The main drawback of this technique is the choice of an appropriate mother wavelet. With inappropriate choices, this technique may not perform well even in high SNR.

We propose a new spike detection algorithm that uses the computation of Cepstrum of Bispectrum (CoB) [14] as an inverse filtering technique. Since the CoB is a higher order statistic (HOS) and because of the inherent properties of higher order statistics, estimates from it are free from the effects of Gaussian background noise. In addition, as the theory of probability underlies the CoB technique, our approach can estimate spikes even from overlapping signals. The algorithm is fully automatic and does not require any prior information about spike shape or even maximum or minimum spike rate. The performance (detection ability) of the proposed algorithm is assessed using synthesized signals and compared with some established algorithms. Finally, we apply the technique to an actual extracellular recording.

2. ALGORITHM DESIGN FOR SPIKE DETECTION

A neurophysiological signal can be modeled as the output of a filtered point process. The signal also contains some other filtered point process data which is noise. Here, the neurophysiological signal $x(t)$ is the convolution of the spike shape with the spike transfer characteristic $s(t)$, integrated over the spiking surface of the neuron. Mathematically, the neurophysiological signal is assumed to be the output of a linear time invariant (LTI) system that can be expressed as

$$x(t) = e(t) \otimes s(t) + w(t) \tag{1}$$

where t is the time index, $e(t)$ is the input point process (Poisson process) and $w(t)$ is the noise which may contain both correlated signals with different amplitudes as well as uncorrelated signals.

Blind equalization theory describes the procedure for restoring the system input signal ($e(t)$) from an unknown LTI systems output signal ($x(t)$). Inverse filtering is one solution for estimating the input signal from filter's output signal. Assume we have a filter $s^{-1}(t)$ (an inverse of $s(t)$) i.e., $s^{-1}(t) \otimes s(t) = \delta(n) = 1$ or in frequency domain $S^{-1}(n)S(n) = 1$ (where n is frequency index). If we apply $x(t)$ (from Eq. 1) to this filter $s^{-1}(t)$, we get an output $z(t)$ as

$$\begin{aligned} z(t) &= x(t) \otimes s^{-1}(t) \\ &= [e(t) \otimes s(t) + w(t)] \otimes s^{-1}(t) \\ &= e(t) \otimes s(t) \otimes s^{-1}(t) + w(t) \otimes s^{-1}(t) \\ &= e(t) + e_w(t) \end{aligned} \tag{2}$$

where $e_w(t)$ is a noise component generated due to noise. The inverse filter's output $z(t)$ should be similar to input signal $e(t)$ of the original process, if $e_w(t)$ is cut-off or attenuated by applying some extra processing to $z(t)$. In the following sections, we describe a technique to estimate the inverse filter blindly from only the output signal $x(t)$, and a procedure to suppress and threshold noise acquired from inverse filter output signal $z(t)$.

2.1 Inverse Filter Estimation

Mathematically, the inverse filter $s^{-1}(t)$ of any invertible linear process can be estimated from its frequency domain transfer function (filter) $S(n)$. We use the CoB based blind filter estimation technique to estimate the system transfer function from the output $x(t)$. The CoB of any LTI process can be computed by applying a 1D inverse Fourier transform operation to the log-Bispectrum:

$$\begin{aligned} c_{B_x}(n,t) &= F_1^{-1}[log\{B_x(n,l)\}] \\ &= F_1^{-1}[log\{\gamma_e S(n)S(l)S^*(n+l)\}]_l \\ &= log\{\gamma_e\}\delta(t) + log\{S(n)\}\delta(t) \\ &\quad + c_s(t) + e^{-j2\pi km/N} c_s(-t) \end{aligned} \tag{3}$$

where $c_{B_x}[\bullet]$ is the CoB of signal $x(t)$, $F_1^{-1}[\bullet]_l$ denotes one dimensional inverse Fourier transform to be applied to the frequency axis l, $B_x(n,l)$ is the bispectrum of $x(t)$, γ_e is the skewness of the input process $e(t)$ and $c_s(t)$ is the cepstrum of the filter $s(t)$. The CoB is a complex measurement which carries both the filter's Fourier magnitude and phase information. As it suppresses any Gaussian noise effects due to the properties of HOS, it is possible to reconstruct filter information blindly from any output signal even in low SNR conditions. The frequency domain filter $S(n)$ of the model neurophysiological signal $x(t)$ can be computed as below:

$$S(n) = \exp[c_{B_x}(n,0) - c_{B_x}(0,0)] \tag{4}$$

The phase unwrapping procedure [14] may need to be applied to Eq. (4). The time domain inverse filter $s^{-1}(t)$ of the model neurophysiological process can be estimated from the frequency domain filter measurement $S(n)$ as below

$$\begin{aligned} S^{-1}(n) &= \frac{1}{S(n)} \\ \text{and} \qquad s^{-1}(t) &= F^{-1}[S^{-1}(n)] \end{aligned} \tag{5}$$

Further details may be found in [14].

2.2 Noise Suppression and Thresholding

Initially we assume the noise amplitude in neurophysiological recordings to be lower than the signal amplitude. Consequently, the amplitude of the noise term at the output of inverse filter ($e_w(t)$ of Eq. (2)) will be lower than the amplitude of associated delta sequence (point process) ($e(t)$). If the the SNR is high, then $e(t)$ can be found using simple amplitude thresholding on Eq. (2). For lower SNR, we can improve on simple amplitude thresholding using additional processing on $z(t)$ to enhance the delta sequence. We denoise the inverse filtered output signal $z(t)$ using the discrete stationary wavelet transformation employing the first coiflet wavelet (coif1) for decomposition and reconstruction. This was chosen because the shape of a delta sequence in a noise free $z(t)$ is very similar to the shape of first coiflet wavelet, whereas noise in $z(t)$ generally has a different shape. Note that the delta sequence found in Eq. (2) is independent of the shape of the neuron spike or additive noise. However, even after denoising in this way, if the delta sequence is not enhanced sufficiently, we use the square or cubic term of the denoised inverse filtered signal.

Setting the amplitude threshold to cut the noise term from the denoised signal is very sensitive: a low threshold level can increase false detection (false positive) while a higher threshold level can increase the number of missing spikes (false negative). In general, the square or cubic function of the denoised inverse filtered signal can enhanced the delta sequence and reduce the noise term. Therefore, setting an appropriate amplitude threshold selection is less difficult in this case. The formula below may be applied to cut out the noise term from the square or cubic function of denoised inverse filtered signal $y(t)$ (where $y(t) = [d_z(t)]^n$; $d_z(t)$ is $z(t)$ denoised using the coiflet wavelet and n is any integer)

$$\theta_y = \frac{1}{N}\sum_{t=1}^{N} y(t) + k * \sigma_y \tag{6}$$

where k is a constant and σ_y is the standard deviation of the signal $y(t)$. The signal above threshold value [i.e. $\hat{e}(t) = \max(0, y(t) - \theta_y)$] may now be used to estimate the delta sequence equivalent to input signal $e(t)$.

3. FINDING SPIKES IN SYNTHESIZED DATA

The performance of the proposed spike detection algorithm is assessed using Monte Carlo trials on synthesized data. Synthetic data is used so that the ground truth is known. Errors

take two forms: missing spikes (false negative) and inserted spikes (false positive).

3.1 Synthesized Neurophysiological Signal

We use the algorithm and code from [15] for generating independent synthesized signals. This models the extracellular signal as a linear mixture of three types of signal:

1. one (or a linear mixture of multiple) target neural spike trains - each spike train is randomly distributed (using a Poisson process but with some minimum inter-spike time interval). The signal is generated by convolving a spike shape with the spike train (a different shape may be used for each target neuron). The shape of the spike is a realistic extracellular spike signal generated from an intracellular signal [15].
2. neural noise - a linear mixture of a few neural spike trains generated by neighboring neurons. The generation of each of these spike signals is similar to the target neural signals. The noise spike trains are highly correlated with the target neural spikes, i.e., the noise spikes appear at around the time of target neuron's spikes.
3. other noise - a set of uncorrelated spike signals (generated in a similar way) and independent identically distributed random signals.

3.2 Signal to Noise Ratio (SNR)

There are a range of techniques for SNR estimation. The instantaneous (power) SNR is the ratio of signal power to background noise power at that instant. It can also be computed from the ratio of the amplitude of the signal to the standard deviation of (zero-mean) background noise. These techniques are most appropriate where the signal is of near-constant amplitude. But in neurophysiology the signal (spike) is highly dynamic. In this case different techniques may be used as discussed by [10, 15]. Following [15] we computed the ratio of the maximum peak to peak amplitudes of the signal and the background noise. To observe the performance of algorithm at different SNRs, we simply manipulate the noise amplitude.

3.3 Performance Evaluation

Extracellular recordings may contain more than one type of spike train. The overall shape of an extracellularly recorded spike is usually biphasic: however, the amplitude and/or duration of each phase differs for different source neurons because of the nature of the conduction path from neuron to electrode. Each experiment involves one or more sets of synthetic neurophysiological signals (1 set = 50 signals) where each signal is 5 seconds long and sampled at 24kHz.

The first experiment uses 6 sets (= 300 signals) of synthetic signals where each signal contains two dominant spike trains with different shapes (Fig. 1). Each set of signals has identical spike trains but the noise amplitude(synthesized using 7 correlated and 15 uncorrelated neurons) is varied. The SNRs used are 0dB, -10dB, -20dB, -30dB, -40dB and -50dB. The firing rate of each spike train is approximately 50Hz ($\pm$5Hz), giving altogether 500 ($\pm$5) spikes in 5 seconds of simulated signal. When comparing detected spikes with ground truth, we allow a tolerance of 0.5ms on each event. Since the amplitude threshold in the proposed technique (discussed in section 2.2) is highly dependent on SNR

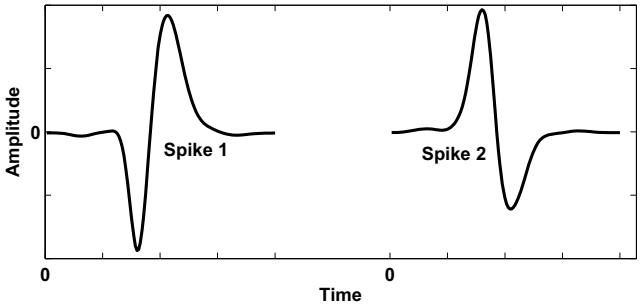

Figure 1: The two spike shapes used to synthesize signals for performance evaluation.

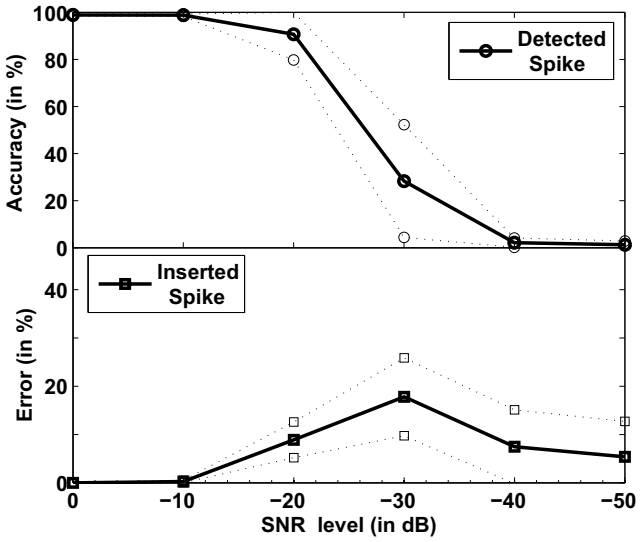

Figure 2: Algorithm Performance showing the spike detection capability and the false positive error (inserted spikes) calculated as a percentage of total actual spikes. The dotted line shows the standard deviation.

value, we tune it so that it minimizes the sum of missing and inserted spike events.

Two performance measures are computed and shown with respect to the percentage of actual spike events: detection and insertion of spikes. The mean detection distribution at different SNRs (Fig 2 top) shows that the algorithm can detect 99% spikes at SNR up to -10dB. In addition, the detection performance is almost same for all signals as the standard deviation is only 0.5% on 50 Monte Carlo tests. The distribution of inserted spikes (Fig 2 bottom) shows that 0.2% insertion errors may occur using this technique and this performance is found on 99.5% of test signals. We note that the algorithm performs better at 0dB or positive SNR.

3.4 Comparison with other techniques

We compare the proposed technique (*cob*) with four established spike detection methods. These are a wavelet based technique (*wav*) [10], a double sided amplitude thresholding technique (*plain*) [3], a morphological filtering based technique (*morph*) [17], and a non-linear energy operator based technique (*neo*) [8]. We programmed the algorithms for the above except for the wavelet based technique, since software

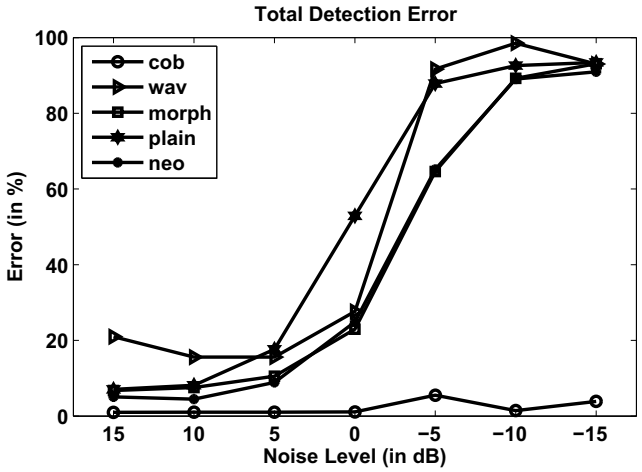

Figure 3: Comparison of five spike detection techniques: the four already established techniques and the *cob* technique. The graph shows the percentage of total (missing and inserted spike) errors.

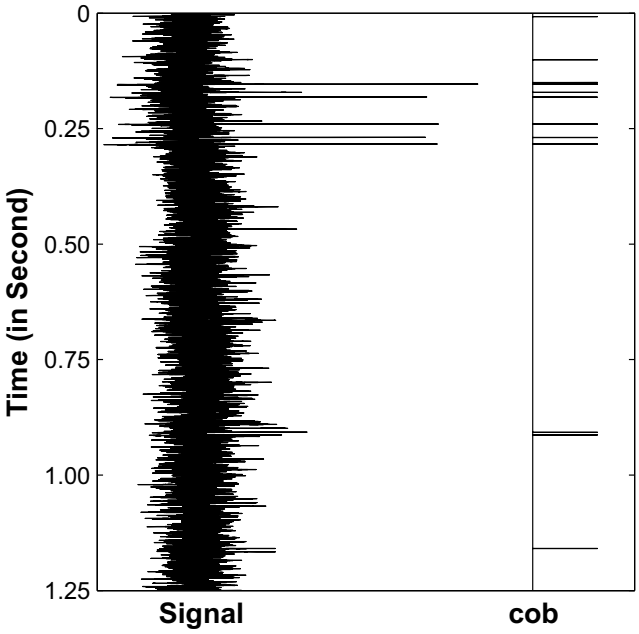

Figure 4: *cob* applied to a segment of a human brain signal acquired from temporal lobe. Only 1.25 second are displayed here. A low threshold ($\theta_y = 0.01$ at normalized y) was used, identifying many spikes.

was provided by Z. Nenadic, author of [10]. We use the same set of signals (containing two dominant spike trains at different noise levels) as described above. All algorithms are applied to each set of signals and the total error computed: missing plus inserted spikes. Since all methods employ amplitude thresholding, we use, as previously, a flexible threshold for each individual method to achieve the minimum total error. Figure 3 compares the performance of all methods,

All methods except *cob* deteriorate rapidly with decreasing SNR when the SNR falls below 0dB. *Wav* shows a high number of failures even at higher SNR. In the case of *Neo*, we observe fewer missed spikes at SNR up to nearly 0dB, but at the same time, a high number of inserted spikes are observed so that the resultant performance is not good at low SNR. The technique *plain* shows the highest failure rate when the signal's SNR is below 10dB. Unlike the other techniques, the total error observed by *cob* is always smaller value in both failure modes. Hence *cob* outperforms the the established techniques on this dataset.

4. FINDING SPIKES IN REAL SIGNALS

Real biomedical signals always differ from synthetic signals. To test our new technique with real signals, we have used a multiunit neurophysiological recording from the temporal lobe of an epileptic patient from Itzhak Fried's lab at UCLA (available at `http://www2.le.ac.uk/departments/engineering/extranet/research-groups/neuroengineering-lab/software`). The signal is 60 seconds long and sampled at 32kHz. Here we have arbitrarily selected a 5 second segment and applied a high pass filter (cut-off frequency 200Hz) to cut out instrumental and electrical artifacts. We apply *cob* to the filtered signal. Fig. 4 shows the algorithm's output. This confirms that the algorithm is suitable for real neurophysiological signals.

The algorithm uses amplitude thresholding in its final stage as described in section 2.2. We, therefore, observe the number of spike events at different thresholds. Fig. 5 shows the number of spikes at different thresholds for this 5 second signal. 10 spikes are found over a wide range of thresholds, but up to 40 may be found by decreasing the threshold. These spikes may be from one or many neurons.

5. DISCUSSION AND CONCLUSION

Extracellular recordings contain single or multiple spike trains plus some correlated and uncorrelated noise. The amplitude of a spike need not be greater than the additive noise (including instrumental/electrical noise). Since a spike signal lasts for 1-2 ms, higher frequency components dominate. Engineers, therefore, use a high sampling frequency to digitize neurophysiological signals and use a high pass filter. Neurophysiological recordings are much longer than single spike signals, which assists higher order statistics estimation. Estimation of the inverse filter is based on cepstrum of bispectrum and this needs a sufficiently large volume of data. We find that processing 50 spikes at a time (here, 5s of data) provides sufficient spike information. The amount of data to be processed at a time can be extended (or reduced) depending on the signal of interest and the frequency of its occurrence: e.g, to observe spikes from in the Delta band of a neurophysiological signal, a longer duration would need to be processed. Note that a large data set may violate the linearity condition for bispectrum estimation.

The proposed technique is independent of sampling frequency: the sampling frequency is required to convert the signal from the time domain to frequency domain. In converting from time to frequency domain the number of samples should be equivalent to least double the duration of a spike shape: here we have used 256 samples throughout.

The critical step in this technique is the estimation of the inverse filter. From previous work [14] CoB can reconstruct any filter (minimum, non-minimum or maximum phase system) information with very low variance from any Poisson

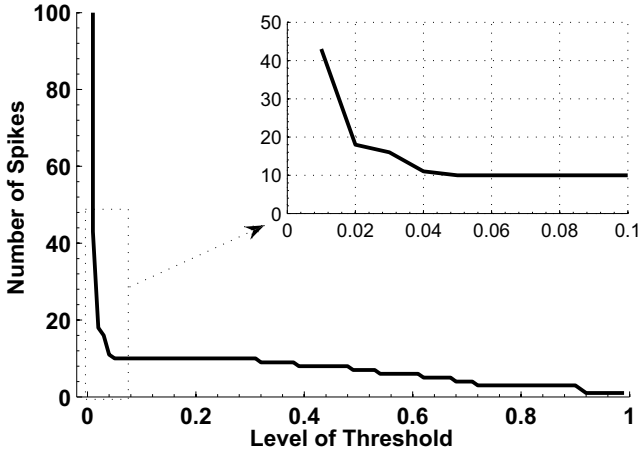

Figure 5: Number of spikes found at different threshold levels.

triggered filter process. Further, CoB can reconstruct the filter from the signal at very low SNR. Hence, we apply the CoB based reconstructed filter to the signal for inverse filtering so that we can find the triggered sequence. We observe in all experiments with synthetic signals that the trigger sequence has been estimated from the signal at SNR below 0dB and it has been possible due to the properties of CoB.

One clear advantage of this algorithm is lowered sensitivity to noise. With the appropriate threshold, CoB does not insert spikes. We found that the established techniques fail on detection and insert events when the test signal's SNR is 0dB or better, whereas the proposed algorithm is free from these errors. The method *plain* detects event without preprocessing and as a result, it is subject to missing and insertion errors. The technique *morph* suppresses noise on the basis of the shape of the spike signal and noise. However it can fail to detect spike events if a spike signal is corrupted by noise and changes its shape. Some noise shapes can be interpreted as false spikes. The technique *wav* use wavelet transformation and its coefficients. The choice of mother wavelet is crucial because the spike shapes may differ considerably and because spikes are corrupted in different ways by noise. Thus *wav* fails to detect some spike signals and can give errors even at high SNR (Fig. 3). The technique *neo* provides the instant non-linear energy without checking the spike shape and, therefore, tends to insert spikes. The method *cob* uses a more sophisticated preprocessing technique which inverts the original convolution. This makes it much more immune to additive noise. This matters because many electrophysiological signals have poor SNR. The proposed technique provides considerable advantages over the other techniques is this case. Future work will use additional real signals, and use receiver operating characteristic (ROC) curves for algorithm assessment.

Acknowledgement

We acknowledge the support of the UK EPSRC, grant number EP/E002331/1 (CARMEN).

REFERENCES

[1] H. Bergman and M.R. DeLong. A personal computer-based spike detector and sorter: implementation and evaluation. *J. Neurosci Methods*, 41:187–197, 1992.

[2] S.M. Bierer and D.J. Anderson. Multichannel spike detection and sorting using an array processing technique. *Neurocomputing*, 26-27:947–956, 1999.

[3] T. Borghi, R. Gusmerol, A. S. Spinelli, and G. Baranauskas. A simple method for efficient spike detection in multiunit recordings. *Journal of Neuroscience Methods*, 163(1):176–180, 2007.

[4] R. Chandra and L.M. Optican. Detection, classification, and superposition resolution of action potentials in multiunit single-channelecordings by an on-line real-time neural network. *IEEE Trans Biomed Eng*, 44:403–412, 1997.

[5] R.C. Gonzalez and P. Wintz. *Digital image processing*. Addison-Wesley, second edition, 1987.

[6] E.V. Goodall and K.W. Horch. Separation of action potentials in multiunit intrafascicular recordings. *IEEE Trans Biomedical Engineering*, 39(3):289–295., 1992.

[7] H. Kaneko, S.S. Suzuki, J. Okada, and M. Akamatsu. Multineuronal spike classification based on multisite electrode recording, whole-waveform analysis, and hierarchical clustering. *Biomedical Engineering, IEEE Transactions on*, 46(3):280–290, 1999.

[8] K.H. Kim and S.J. Kim. Neural spike sorting under nearly 0-db signal-to-noise ratio using nonlinear energy operator and artificial neural-network classifier. *IEEE Trans. Biomed. Eng.*, 47(10):1406–1411, 2000.

[9] N. Mtetwa and L. S. Smith. Smoothing and thresholding in neuronal spike detection. *Neurocomputing*, 69(10-12):1366–1370, 2006.

[10] Z. Nenadic and J.W. Burdick. Spike detection using continuous wavelet transform. *IEEE Trans Biomed Eng*, 52(1):74–87, 2005.

[11] I. Obeid and P.D. Wolf. Evaluation of spike detection algorithms for a brain-machine interface application. *IEEE Trans biomed eng*, 51(6):905–911, 2004.

[12] C.F Olson. Maximum-likelihood image matching. *IEEE Trans Pattern Analysis and Machine Intelligence*, 24(6):853–857, 2002.

[13] E. M. Schmidt. Computer separation of multi-unit neuroelectric data: a review. *Journal of Neuroscience Methods*, 12(2):95–111, 1984.

[14] S. Shahid and J. Walker. Cepstrum of bispectrum: a new approach to blind system reconstruction. *Signal Processing*, 88(1):19–32, 2008.

[15] L. S. Smith and N. Mtetwa. A tool for synthesizing spike trains with realistic interference. *Journal of Neuroscience Methods*, 159(1):170–180, 2007.

[16] L.S. Smith, S. Shahid, A. Vernier, and N. Mtetwa. Finding events in noisy signals. In *Proc. of Irish Signals and Systems Conference*, pages 31–35, 2007.

[17] G. Xu, J. Wang, Q. Zhang, S. Zhang, and J Zhu. A spike detection method in eeg based on improved morphological filter. *Computers in Biology and Medicine, Volume 37, Issue 11, November 2007, Pages 1647-1652*, 37(11):1647–1652, 2007.